

1
2
3
4
5
6
7
8
9
10
11
12
13
14
15
16
17
18
19
20
21
22
23
24

A reply to Comment on “An experimental study of symmetry lowering of analcime”

Atsushi Kyono

Division of Earth Evolution Sciences, Graduate School of Life and Environmental Sciences,
University of Tsukuba, 1-1-1 Tennodai, Tsukuba, 305-8572, Japan

Corresponding author: A. Kyono
Email: kyono@geol.tsukuba.ac.jp
Phone: +81-29-853-7176
Fax: +81-29-853-7887
orcid.org/0000-0001-5419-390X

25

Abstract

26 The symmetry lowering of analcime reported by Sugano and Kyono (2018) was re-investigated
27 by using field-emission scanning electron microscopy. The results of scanning electron microscopic
28 observation show the fractures can be characterized by smoothly curved surfaces, called sub-
29 conchoidal fracture, and neither the lamellar twin nor the domain walls of twin was found on the
30 surfaces of the analcimes. In addition, the lamellar twin is generally formed by transformation from
31 the high-temperature phase or from pseudomorphic replacement under strong alkaline conditions.
32 Actually, the symmetry lowering of analcime reported by Sugano and Kyono (2018) occurs at 200 °C.
33 The temperature is a much lower than the transformation from the high-temperature phase. In the
34 hydrothermal experiment (Sugano and Kyono 2018), moreover, the analcimes were synthesized under
35 acidic condition and reheated in pure water. No twin domain is likely to be formed under the
36 hydrothermal condition. These facts strongly deny the possibility that the twin domains cause the
37 pseudo-symmetry of tetragonal analcime. Consequently, it can be concluded that the observed
38 forbidden reflections for the cubic *Ia3d* symmetry is not due to the presence of twin domains, but due
39 to the symmetry lowering of analcime from cubic *Ia3d* to orthorhombic *Ibca*.

40

41 **Keywords:** analcime, hydrothermal treatment, SEM, fracture surface

42

43 The crystal structure of analcime, ideal chemical formula $\text{NaAlSi}_2\text{O}_6 \cdot \text{H}_2\text{O}$, is composed of a
44 three dimensional framework of SiO_4 and AlO_4 tetrahedra with the ANA-type topology (Baerlocher
45 et al. 2007). The maximum symmetry of the ANA framework is cubic with space group $Ia3d$, but
46 naturally occurring analcimes possess at least four different symmetries: cubic space group $Ia3d$,
47 tetragonal space group $I4_1/acd$, orthorhombic space group $Ibca$, and monoclinic space group $I2/a$
48 (Ferraris et al. 1972; Mazzi and Galli 1978; Hazen and Finger 1979; Pechar 1988). It has long been
49 recognized that the symmetry lowering of analcime from cubic $Ia3d$ to orthorhombic $Ibca$ is caused
50 by the ordering of Si and Al cations in the framework T sites (Mazzi and Galli 1978). Recently, we
51 reported that the hydrothermal heating of analcime influences the degree of ordering of Si and Al over
52 the framework T sites, which lowers its symmetry from cubic $Ia3d$ to orthorhombic $Ibca$ (Sugano and
53 Kyono 2018). In the comment on “An experimental study of symmetry lowering of analcime”
54 (Nespolo 2018), however, the author points out that the reheated analcimes are not orthorhombic $Ibca$
55 but tetragonal $I4_1/acd$. The author mentions that the presence of twin domains is extremely probable
56 because of the pronounced cubic pseudo-symmetry of tetragonal analcime. As it is well known, fine
57 lamellar on $\{110\}$ is present as a pseudo-merohedral twinning in the non-cubic analcimes (Deer et al.
58 2004). The lamellar twin texture observed in the analcimes ranges from several tens of micrometers
59 down to approximately 100 nm (Xia et al. 2009). Therefore, if the “pseudo-single crystal” of analcimes
60 is composed of the twin domains with different orientations, it is observable by electron microscopy.
61 In the paper we report on the observation of fracture surfaces by field-emission scanning electron
62 microscopy (FE-SEM, JEOL JSM-IT300HR).

63 Figure S1A shows the lamellar domains of analcime covered on the surface (Xia et al. 2009).
64 Figures S1B to D display the representative fracture surfaces of hydrothermally treated analcime
65 grains (Sugano and Kyono 2018). The fractures of analcime single crystals used in Sugano and Kyono
66 (2018) can be characterized by smoothly curved surfaces, called sub-conchoidal fracture. It is usually

67 found in naturally occurring analcime (Anthony et al. 2004). Neither the lamellar twin nor the domain
68 walls of twin has been, however, found on the surfaces of these analcimes. This result denies the
69 possibility that the presence of twin domains leads to the pseudo-symmetry of tetragonal analcime.

70 In addition, the fine lamellar is considered due to transformation from the high-temperature
71 phase (Coombs 1955; Liou 1970; Takéuchi et al. 1979). These authors described that the
72 transformation takes place above at least temperatures exceeding 300 °C. The symmetry lowering of
73 analcime (Sugano and Kyono 2018), however, occurs at 200 °C. The temperature is a much lower than
74 the transformation from the high-temperature phase. Although the fine lamellar texture of analcime
75 occurs at 210 °C by hydrothermal treatment (Xia et al. 2009), it exhibits a strong pH-dependent. The
76 formation of twin domains favor the strong alkaline conditions, whereas in the hydrothermal
77 experiment (Sugano and Kyono 2018), the analcimes were synthesized under acidic condition and
78 reheated in pure water. These facts also deny the possibility that the twin domains causes the pseudo-
79 symmetry of tetragonal analcime. Therefore, no twin domain is present in the analcimes used in
80 Sugano and Kyono (2018). That is, the observed forbidden reflections for the cubic *Ia3d* symmetry is
81 not ascribed to the presence of twin domains, but to the symmetry lowering of analcime. Based on the
82 all results of single-crystal XRD measurements and SEM observation, it can be concluded that the
83 hydrothermal heating of analcime influences the degree of ordering of Si and Al over the framework
84 *T* sites, leading to the phase transformation from cubic *Ia3d* to orthorhombic *Ibca*.

85

86 **References**

- 87 Anthony JW, Bideaux RA, Bladh KW, Nichols MC (eds) (2004) Handbook of mineralogy,
88 mineralogical society of America, Chantilly, VA 20151-1110, USA;
89 <http://www.handbookofmineralogy.org/>
- 90 Baerlocher CH, McCusker LB, Olson DH (2007) Atlas of zeolite framework types. pp. 398, Elsevier,

91 Amsterdam

92 Coombs DS (1955) X-ray observations on wairakite and non-cubic analcime. *Mineral Mag* 30:
93 699–708

94 Ferraris G, Jones DW, Yerkess J (1972) A neutron-diffraction study of the crystal structure of analcime,
95 $\text{NaAlSi}_2\text{O}_6 \cdot \text{H}_2\text{O}$. *Z Kristallogr* 135:240–252

96 Deer WA, Howie RA, Wise, WS, Zussman J (2004) *Rock-forming minerals*, 4B, Framework silicates:
97 silica minerals, feldspathoids and the zeolites. pp. 982, Geological Society of London.

98 Hazen RM, Finger LW (1979) Polyhedral tilting: A common type of pure displacive phase transition
99 and its relationship to analcime at high pressure. *Phase Transitions*, 1:1–22

100 Liou JG (1970) Synthesis and stability relations of wairakite, $\text{CaAl}_2\text{Si}_4\text{O}_{12} \cdot 2\text{H}_2\text{O}$. *Contr Mineral Petrol*,
101 27:259–282

102 Mazzi F, Galli E (1978) Is each analcime different? *Am Mineral* 63:448–460

103 Nespolo M. (2018) Comment on “An experimental study of symmetry lowering of analcime”. *Phys*
104 *Chem Miner* (to be submitted)

105 Pechar F (1988) The crystal structure of natural monoclinic analcime ($\text{NaAlSi}_2\text{O}_6 \cdot \text{H}_2\text{O}$). *Z Kristallogr*
106 184:63–69

107 Sugano N, Kyono A (2018) An experimental study of symmetry lowering of analcime. *Phys Chem*
108 *Miner* (to be submitted)

109 Takéuchi Y, Mazzi F, Haga N, Galli E (1979) The crystal structure of wairakite. *Am Mineral*,
110 64:993–1001.

111 Xia F, Brugger J, Ngothai Y, O'Neill B, Chen GR, Pring A (2009) Three-dimensional ordered arrays
112 of zeolite nanocrystals with uniform size and orientation by a pseudomorphic coupled
113 dissolution-reprecipitation replacement route. *Cryst Growth Des*, 9:4902–4906

114

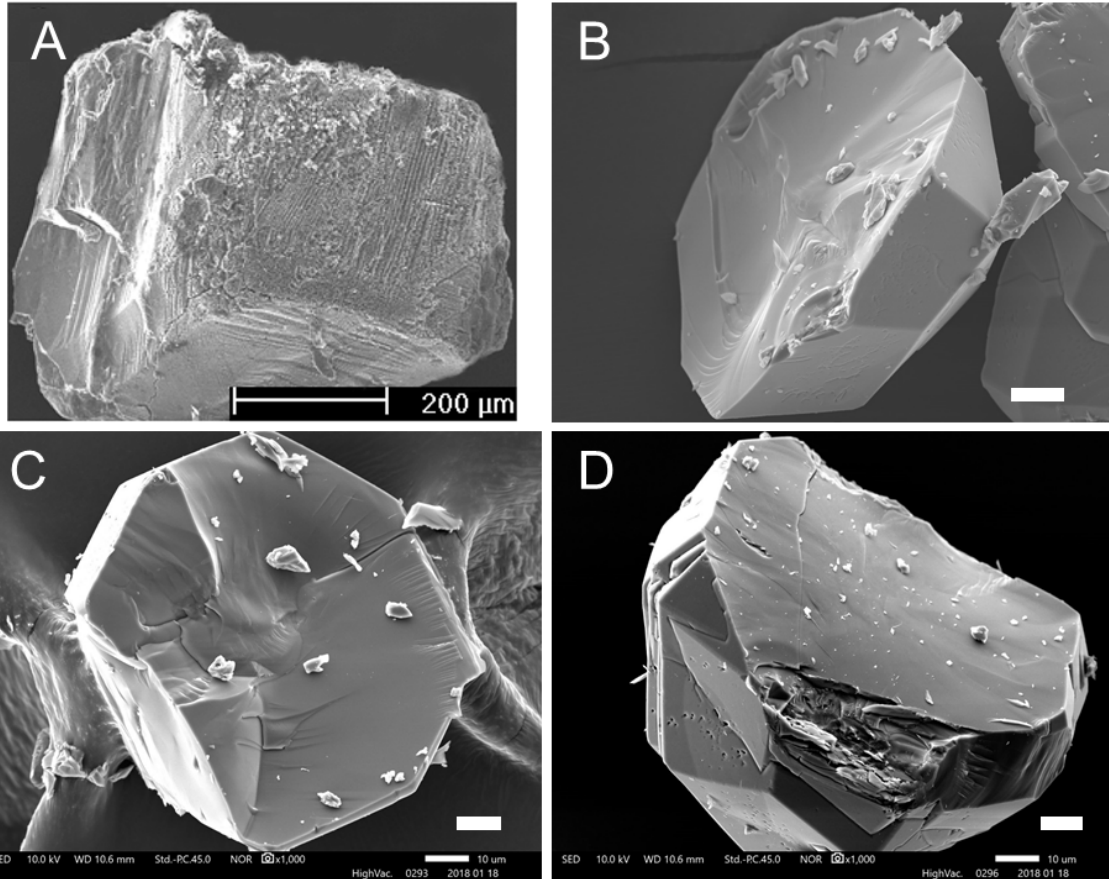
Captions for Figures and Tables

115

116

117 **Figure S1** (A) The lamellar twin texture of analcime covered on the surface reported by Xia et al.
118 (2009). Fracture surfaces of analcime single crystal (B) used as a starting material by
119 Sugano and Kyono (2018), (C) reheated hydrothermally for 24 h, and (D) for 48 h. Scale
120 bar = 10 μm .

121



122

123 **Figure S1** (A) The lamellar twin texture of analcime covered on the surface reported by Xia et al.

124 (2009). Fracture surfaces of analcime single crystal (B) used as a starting material by

125 Sugano and Kyono (2018), (C) reheated hydrothermally for 24 h, and (D) for 48 h. Scale

126 bar = 10 μm .

127